ELSEVIER

International Journal of Mass Spectrometry 176 (1998) 23–38

Ab initio calculations on the isomerization of the benzene radical cation to the Dewar benzene structure and on possible pathways for the formation of C_4H_4 fragment ions from the benzene radical cation

W.J. van der Hart

Leiden Institute of Chemistry, Gorlaeus Laboratories, Leiden University, P.O. Box 9502, 2300 RA Leiden, The Netherlands

Received 17 November 1997; accepted 22 January 1998

Abstract

Ab initio calculations of possible fragmentation pathways for the formation of C_4H_4 fragment ions from the benzene radical cation show that the dissociation of lowest energy leads to the methylene cyclopropene radical cation. The calculated barriers for formation of the other classical C_4H_4 ion structures, vinyl acetylene, cyclobutadiene, and butatriene, are about 10 kcal mol^{-1} higher and almost identical. The fact that, in fragmentations of C_6H_6 precursors, besides the methylene cycloprene ion, only the vinyl acetylene ion is observed, should be ascribed to the fact that formation of this ion structure is much more direct than a fragmentation to the cyclobutadiene or the butatriene ion structure. (Int J Mass Spectrom 176 (1998) 23–38) © 1998 Elsevier Science B.V.

Keywords: Ab initio calculations; Dewar benzene radical cation; Fragmentation of C_6H_6 radical cations; C_4H_4 fragment ions

1. Introduction

In a recent review on the calculation of unimolecular decay rates [1], Baer called the dissociation of the benzene radical cation, as observed in mass spectrometry, a simple and complex story. The reason for this statement is that both the dissociation thresholds and the dissociation rates are known rather accurately but that essentially nothing is known about the dissociation mechanisms.

From many studies on the structures of C_4H_4 fragment ions from different precursors, it is now generally assumed that the fragment ions observed in the mass spectra of benzene and of many of its isomers are a mixture of methylene cyclopropene and vinyl acetylene radical cations (see [2] and [3] and references cited therein). The other classical ion structures, butatriene and cyclobutadiene, can only be formed from precursors having structures that are more or less prepared for the production of these fragment ions.

In previous articles from this laboratory, we have discussed quantum chemical calculations on the isomerization of C_6H_6 [4–8] and C_4H_4 [9] radical cations. From this work it appeared that there are many isomerization barriers below the dissociation limit in the potential energy surface of C_6H_6 radical cations. The lowest barrier found in the potential energy surface of C_4H_4 radical cations was that for an isomerization of the nonclassical CH_2CCHCH radical

PII S1387-3806(98)14009-5

Table 1
Energies at the ROHF//6-31G** level of the benzene radical cation and the sum of the energies of the ethyne molecule and the classical C_4H_4 fragment ions in Hartree and as the relative energies in kcal mol^{-1}. These latter values are not corrected for differences in zero-point energy

	Energy	ΔE
Benzene$^{\cdot+}$	−230.421222	0
Methylene cyclopropene$^{\cdot+}$ + C_2H_2	−230.268853	95.6
Vinyl acetylene$^{\cdot+}$ + C_2H_2	−230.234038	117.5
Cyclobutadiene$^{\cdot+}$ + C_2H_2	−230.240305	113.5
Butatriene$^{\cdot+}$ + C_2H_2	−230.228811	120.7

cation to the structure of lowest energy, the methylene cyclopropene radical cation. The energy of this non-classical ion was calculated to be 30 kcal mol^{-1} higher than that of the methylene cyclopropene ion and the barrier for its isomerization only 6 kcal mol^{-1}. All other barriers were found to be at least 2.4–2.5 eV above the energy of the methylene cyclopropene ion. These results, together with the previous experiments [2,3], make it very unlikely that isomerization of a C_4H_4 radical cation will take place after the fragmentation process. This means that differences in observed structures of C_4H_4 fragment ions should be ascribed to isomerizations of the precursor ion prior to fragmentation. In [9] we have made some suggestions about the possible pathways for formation of C_4H_4 ion structures from C_6H_6 precursor ions. In the present work, these possible pathways and some alternatives are studied by ab initio calculations.

2. Methods

Ab initio calculations that use the 6-31G** basis set were performed with both the GAMESS-UK [10] and the Gaussian 94 [11] program packages. In previous calculations on the isomerization of C_3H_4 radical cations [12], it was found that at crucial points

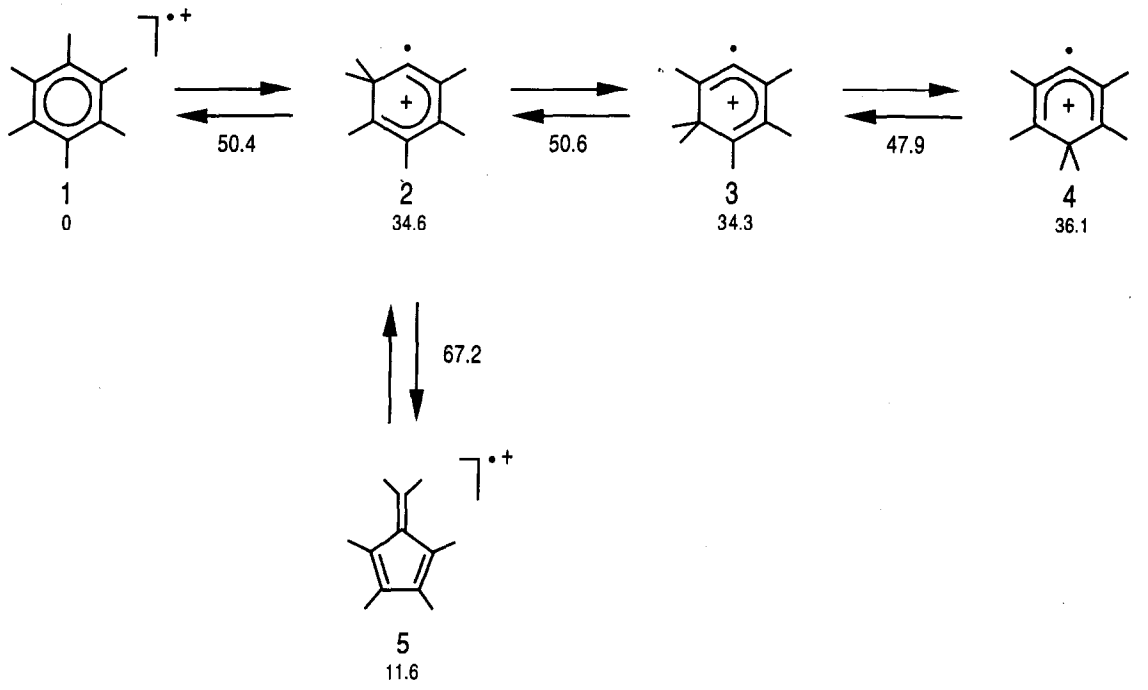

Fig. 1. Reaction scheme for carbon and hydrogen scrambling in the benzene radical cation with the relative energies in kcal mol^{-1} [5]. The relative energies of the transition states can be slightly different from the values in [6–8] because of a small difference in the selection threshold in the Table CI calculations.

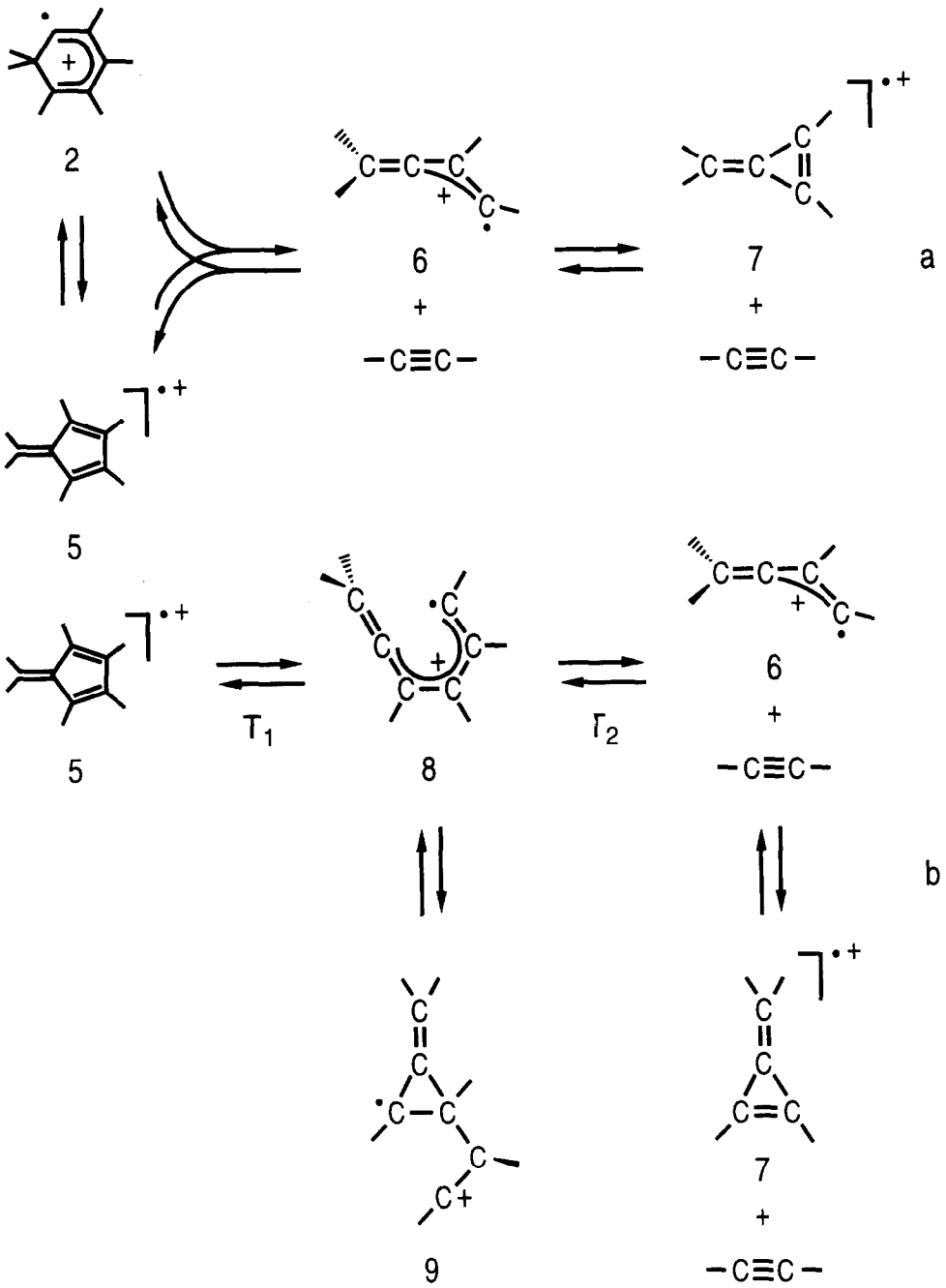

Fig. 2. (a) Reaction scheme previously suggested [9] for the production of the methylene cyclopropene fragment ion. (b) Extension of the scheme in (a) (see text).

Table 2
ROHF, MRCI, and ZPE energy values in Hartree for part of the radical cation structures and transition states in Fig. 2 and relative energies with respect to the benzene structure in kcal mol^{-1}. The latter values are obtained from the MRCI energies corrected for the ROHF zero-point energies scaled by a factor of 0.89. Further details of the ion structures in this and the other tables (geometries, vibrational frequencies) can be obtained from the author

	ROHF	ZPE	MRCI	ΔE
Benzene $\mathbf{1}^{\cdot+}$ [a]	−230.421222	0.105319	−230.868588	0
Fulvene $\mathbf{5}^{\cdot+}$ [a]	−230.401340	0.104267	−230.849193	11.6
T_1 [a]	−230.286671	0.099070	−230.741823	76.1
Structure **8** [a]	−230.298365	0.099127	−230.742959	75.4
Structure **9**	−230.211163	0.095969	−230.654886	128.9
T_2	−230.213082	0.094099	−230.655646	127.4

[a]Values taken from [5] and [7].

Table 3
ROHF, MRCI, and ZPE energy values in Hartree for the radical cation structures and transition states in Figs. 3 and 4 and relative energies with respect to the benzene structure in kcal mol^{-1}. The latter values are obtained from the MRCI energies corrected for the ROHF zero-point energies scaled by a factor of 0.89

	ROHF	ZPE	MRCI	ΔE
Benzene $\mathbf{1}^{\cdot+}$ [a]	−230.421222	0.105319	−230.868588	0
Structure **2** [a]	−230.369397	0.104552	−230.812758	34.6
T_3	−230.257017	0.100472	−230.710247	96.7
Structure **10**	−230.306132	0.100566	−230.732798	82.6
T_4	−230.242825	0.095694	−230.691950	105.5
11, minimum	−230.276940	0.094729	−230.701402	99.0
10 Å	−230.269231	0.094071	−230.694804	102.8
15 Å	−230.268963	0.094048	−230.694512	102.9

[a]Values taken from [5].

on the potential energy surface an unrestricted Hartree–Fock (UHF) calculation may produce unacceptable values for the spin angular momentum $\langle S^2 \rangle$ as high as 1.0. For this reason stable ion structures and transition states were optimized at the restricted open shell Hartree-Fock (ROHF) level. Transition states were tested by a calculation of the vibrational frequencies and by a visualization of the vibration corresponding with the single negative force constant by use of VIBRAM [13]. In some cases, transition states were also tested by intrinsic reaction coordinate (IRC) calculations. For the optimized structures, multireference configuration interaction (MRCI) calculations with single and double excitations were done with the Table CI ([14] and references cited therein) option of GAMESS-UK. In these calculations excitations involving the lowest 10 occupied and the highest 40 virtual molecular orbitals were not included (these latter orbitals have an orbital energy higher than 2 Hartree). All configurations having a coefficient squared higher than 0.0025 in the final ground state wave function or higher than 0.0030 in the wave function for the second root (of the same symmetry) were used as reference configurations. The selection threshold used in Table CI was set at 7.5 μHartree, the lowest value compatible with the maximum number of 30,000 configurations in the final diagonalization. In Table CI calculations the contribution of the

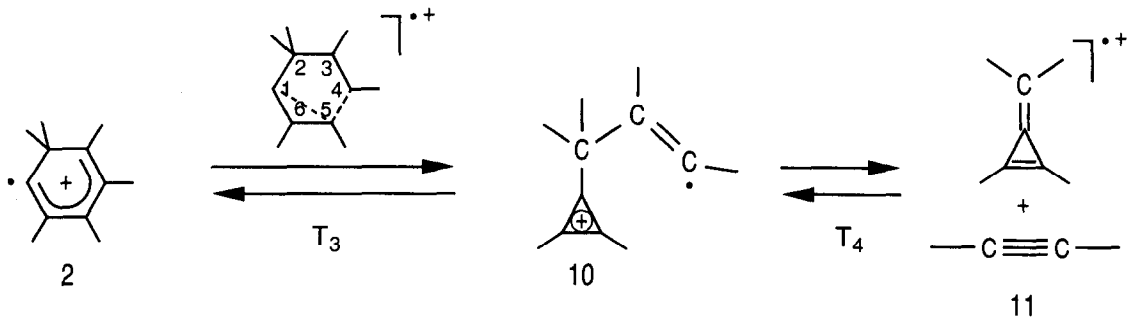

Fig. 3. Alternative reaction scheme for the production of the methylene cyclopropene fragment ion.

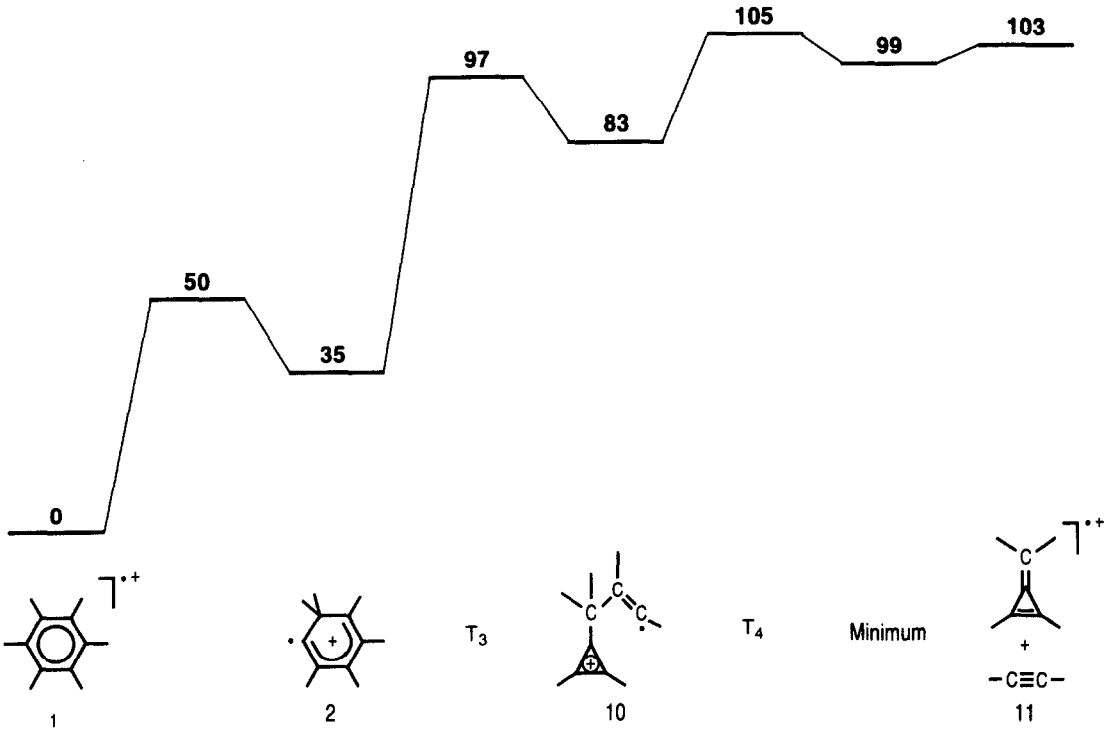

Fig. 4. Energy diagram for the fragmentation to the methylene cyclopropene structure. The relative energies are in kcal mol^{-1}.

remaining configurations is calculated by perturbation theory. The MRCI values given in Table 1 include a generalized Davidson size-consistency correction [15].

In a few cases the transition state optimizations were combined with CASSCF (complete active space SCF) calculations where the active space had seven electrons in eight orbitals.

A first optimization that used a 4-31G basis set of T_6 (Fig. 6) did not produce an acceptable geometry and an additional IRC (intrinsic reaction coordinate) calculation did not show a connection of this geometry with structures **3** and **14**. We assumed that the start geometry of this optimization was too far from the correct geometry to have the unpaired electron on the correct carbon atom. For this reason, the calculation was repeated at the CASSCF level. This produced a much more acceptable geometry with a correct behavior in additional IRC calculations. Because the CASSCF wave functions were relatively close to a single Slater determinant, further calculations on this transition state were again done at the ROHF level.

In the ROHF geometries of T_7 (Fig. 6) and T_{12} (Fig. 12), the C_2H_2 fragment was in an essentially symmetric position perpendicular to the C_4H_4 unit. As a result, an IRC calculation on T_{12} did not go to **19** but to a very unstable structure where the acetylene fragment was bonded to the butatriene unit via a three-membered ring. In both cases, the CASSCF calculation produced a somewhat less symmetric structure but, also here, the wave functions were close to a single Slater determinant and the energies at the ROHF level were not significantly different from those obtained from the ROHF calculations. In order to keep all results as comparable as possible, further calculations were, therefore, based on the ROHF geometries.

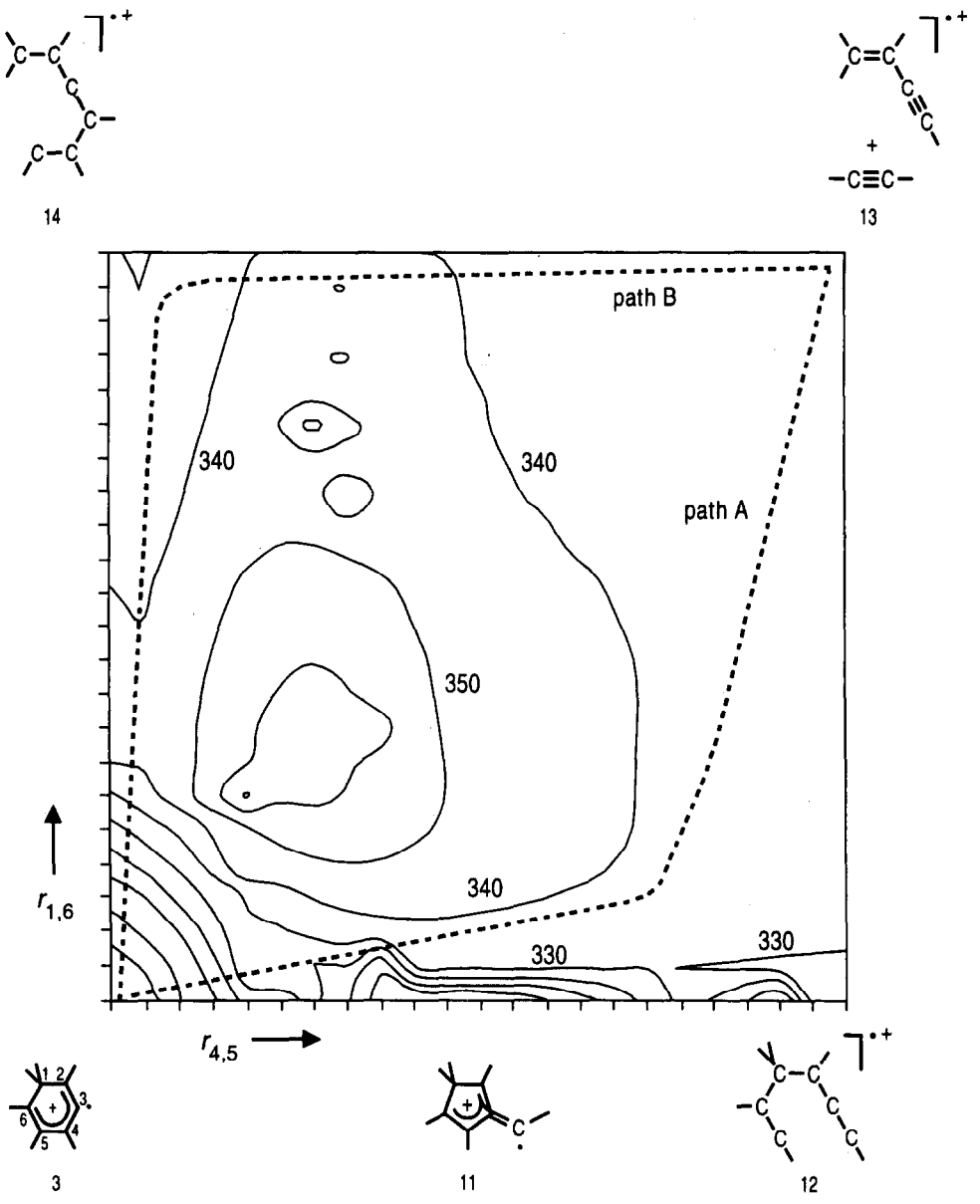

Fig. 5. Semiempirical potential energy surface (kcal mol^{-1}) for the formation of the vinyl acetylene fragment ion **13** from structure **3**. The distances between the contour lines are 10 kcal mol^{-1}.

3. Results and discussion

As suggested in [9], the methylene cyclopropene and vinyl acetylene radical cations can, in principle, be formed by fragmentation of the ion structures that are responsible for carbon and hydrogen scrambling in the benzene radical cation. As shown in Fig. 1, taken from [5], the barriers for these scrambling processes are significantly below the lowest dissociation barrier of the benzene radical cation (formation of the phenyl cation), which is given as 3.66 eV = 84 kcal mol^{-1} in [16] and as 3.88 eV = 89 kcal mol^{-1} in

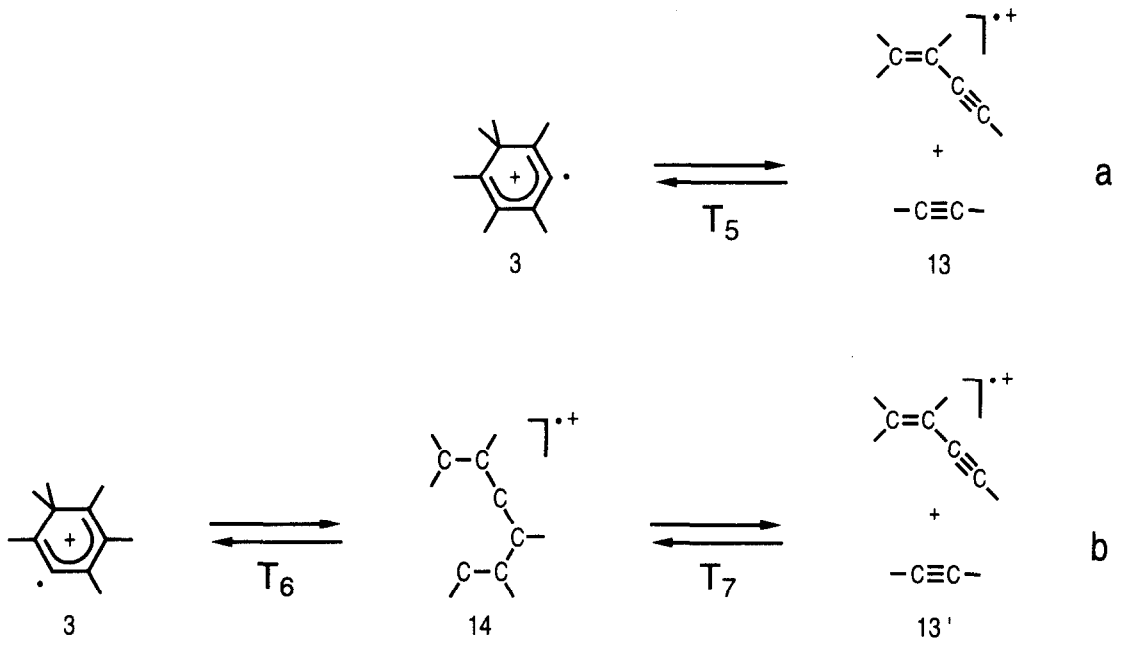

Fig. 6. Reaction schemes for the production of the vinyl acetylene fragment ion.

[17]. Both of these values are obtained from fits of experimental data by using Rice–Ramsperger–Kassel–Marcus (RRKM) theory.

For the formation of the other classical C_4H_4 radical cation structures, cyclobutadiene, and butatriene, more complicated processes are needed. The only reasonable precursor for the fragmentation to the butatriene structure is probably the dimethylene cyclobutene radical cation, which can be obtained from the benzene structure by a series of rearrangements. The lowest barrier in this pathway is calculated to be close to the dissociation limit of the benzene radical cation, but sufficiently low for an isomerization without decomposition [7]. In a similar way, formation of the cyclobutadiene structure seems only possible after an isomerization of the benzene radical cation to the Dewar benzene structure. This rearrangement, which has not been described in previous articles, will be considered below.

In the following sections all of these processes and

Table 4
ROHF, MRCI, and ZPE energy values in Hartree for the radical cation structures and transition states in Figs. 5–7 and relative energies with respect to the benzene structure in kcal mol^{-1}. The latter values are obtained from the MRCI energies corrected for the ROHF zero-point energies scaled by a factor of 0.89

	ROHF	ZPE	MRCI	ΔE
Benzene **1**$^{\cdot+}$ [a]	−230.421222	0.105319	−230.868588	0
Structure **3**[a]	−230.365100	0.104318	−230.812943	34.4
Structure **12**	−230.235128	0.096089	−230.675969	115.7
T_5	−230.230054	0.095781	−230.684466	110.2
13, minimum	−230.241856	0.095241	−230.684593	109.8
10 Å	−230.234351	0.093938	−230.676145	114.4
15 Å	−230.234129	0.093912	−230.676219	114.3
T_6	−230.236218	0.099319	−230.709106	96.7
Structure **14**	−230.283455	0.099086	−230.721536	88.8
T_7	−230.233172	0.095473	−230.690080	106.5
13', minimum	−230.242239	0.094734	−230.686616	108.3
10 Å	−230.234321	0.093933	−230.678411	113.0
15 Å	−230.234125	0.093910	−230.678314	113.0

[a]Values taken from [5].

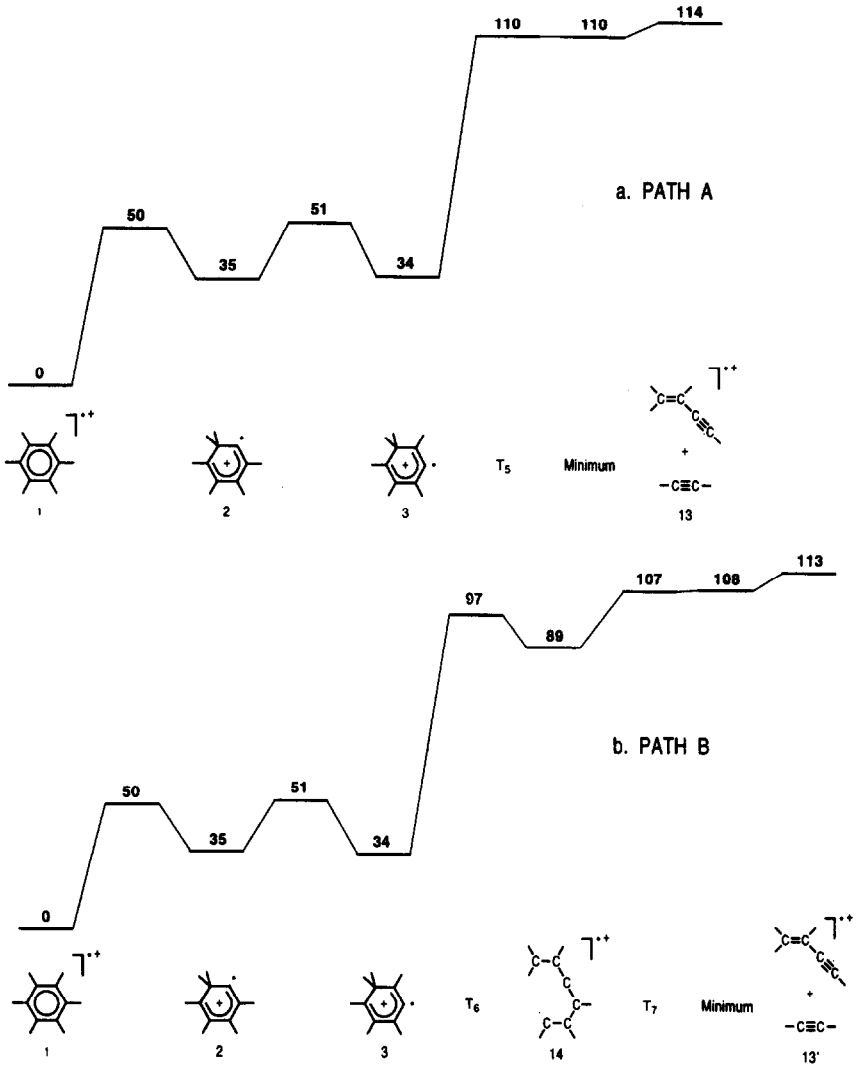

Fig. 7. Energy diagrams for the production of the vinyl acetylene fragment ion via path A and B, respectively. The relative energies are in kcal mol^{-1}.

some alternatives will be discussed in detail. The results will be compared with the experimental value for the dissociation limit for the formation of C_4H_4 radical cations, which is given as 4.16 eV = 96 kcal mol^{-1} in [16].

3.1. Possible fragmentation pathways to the methylene cycloprene structure

In [9], it has been suggested that the methylene cyclopropene ion can be formed by a breaking of two C–C bonds in either the fulvene structure **5** or structure **2** in Fig. 1 followed by an isomerization of the resulting nonclassical ion structure **6** to the methylene cyclopropene structure **7** [see Fig. 2(a)]. As mentioned above, the barrier for an isomerization of structure **6** to the methylene cyclopropene structure was calculated to be only 6 kcal mol^{-1} but the energy of structure **6** was found to be 30 kcal mol^{-1} higher than that of the methylene cyclopropene radical cation [9]. Ab initio calculations at the ROHF//6-31G**

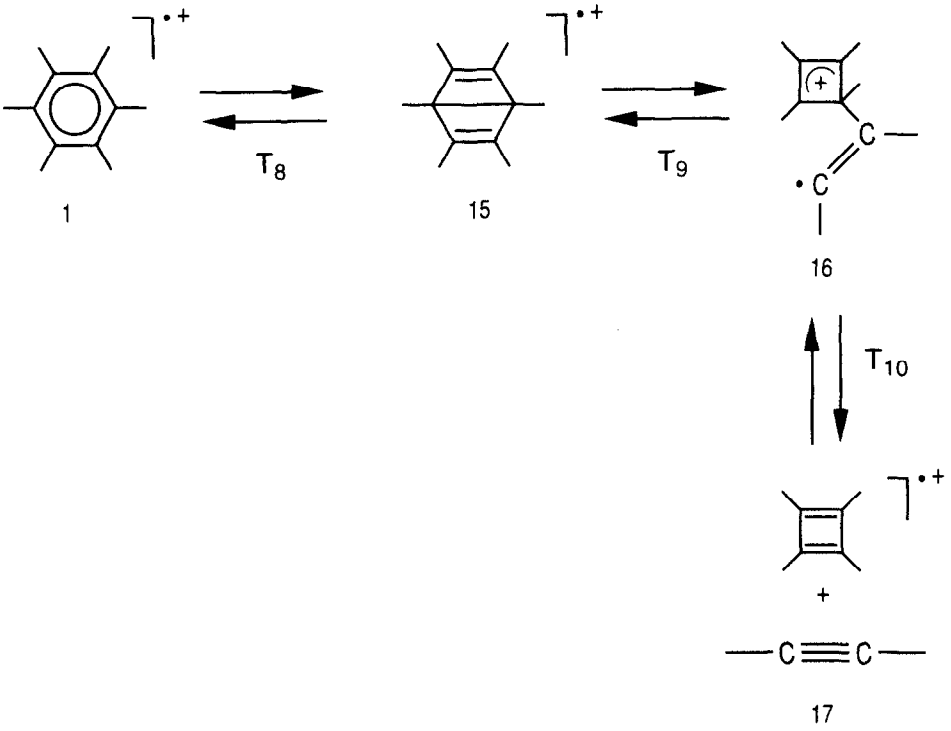

Fig. 8. Reaction scheme for the fragmentation to the cyclobutadiene radical cation.

level on the benzene and methylene cyclopropene radical cations and on neutral ethyne produce the energy values given in Table 1. The energy difference between the benzene radical cation and a combination of the methylene cyclopropene fragment ion plus the ethyne molecule of 95.6 kcal mol^{-1} is very close to the experimental dissociation limit of 96 kcal mol^{-1} given by Kühlewind et al. [16]. This result makes it rather unlikely that structure **6** is an intermediate in the formation of the methylene cyclopropene fragment ion. It follows that the fragmentation pathway shown in Fig. 2(a) is only possible if the isomerization of structure **6** takes place before the fragments go apart. For this reason, we have extended the reaction scheme in Fig. 2(a) to that shown in Fig. 2(b). In this latter scheme we have not included structure **2**. The reason is that the barrier for an isomerization of structure **8** to the fulvene structure **5** is very low and significantly above the barrier for a further isomerization to structure **2** (Table 2). Semiempirical calculations also show a connection of structure **8** with the valley between structure **2** and the fulvene structure. The relative energies in Table 2 show that both the values for structure **9** (129 kcal mol^{-1}) and for the transition state T_2 for a bond breaking in structure **8** (127 kcal mol^{-1}) are significantly above the experimental dissociation limit of 96 kcal mol^{-1} mentioned above. Our conclusion, therefore, is that the reaction schemes given in Fig. 2 are not acceptable as possible dissociation pathways.

For this reason, we have considered the alternative reaction scheme shown in Fig. 3, where in the intermediate structure **10** the leaving HCCH unit is bonded to the CH_2 group of the methylene cyclopropene radical cation. Structure **10** is characterized by an "aromatic" charged three-membered ring and has the unpaired electron in a localized σ orbital. It is therefore not surprising that its heat of formation (Table 3) is calculated to be significantly lower than that of structure **9** (Table 2).

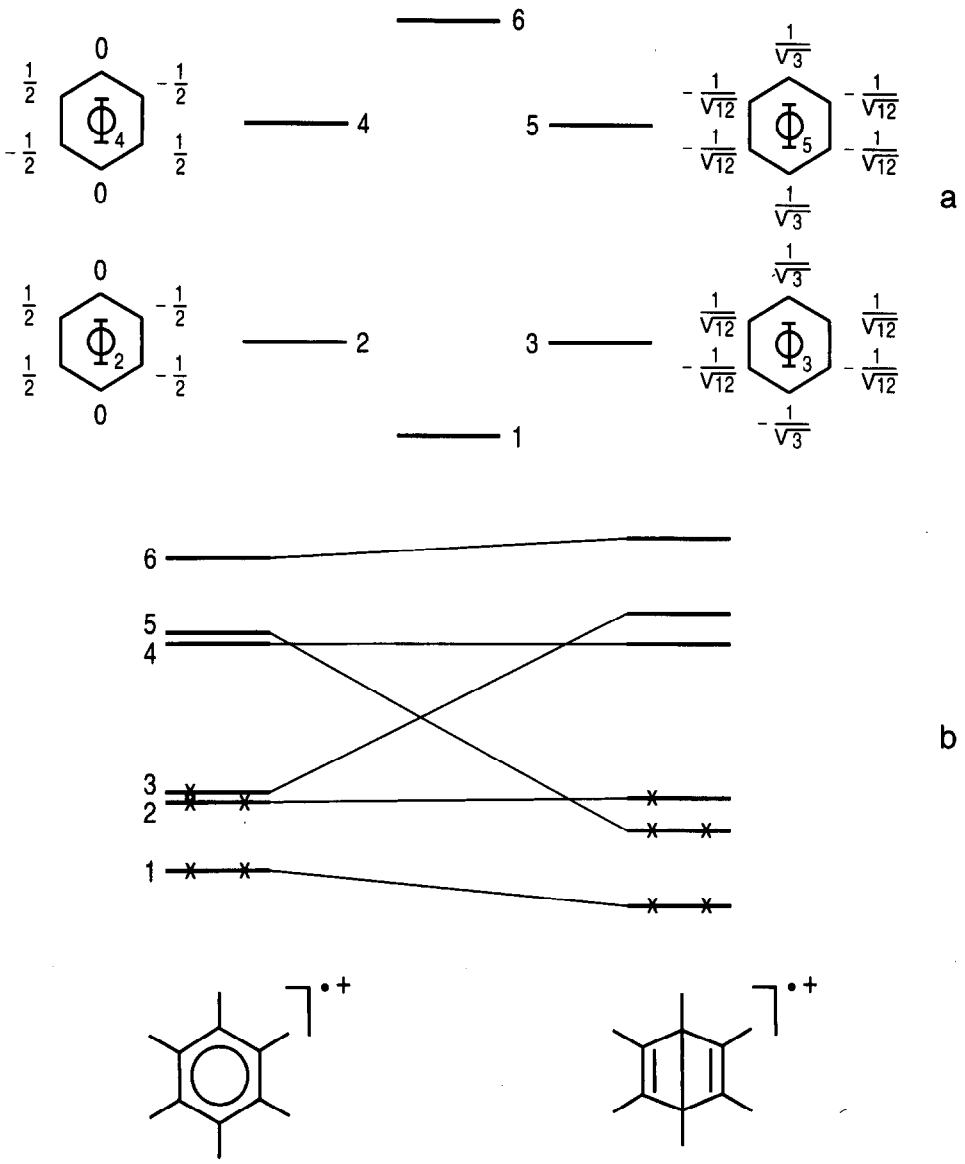

Fig. 9. (a) π-electron molecular orbitals for the benzene radical cation. (b) Molecular orbital correlation diagram for the rearrangement of the benzene radical cation to the Dewar benzene structure.

A semiempirical grid calculation in which the C_1–C_5 and C_4–C_5 distances in structure **2** were varied gave an indication that a direct rearrangement of structure **2** to structure **10** is possible. Ab initio calculations on the basis of these semiempirical results indeed produced an acceptable structure for T_3. A calculation of the force constants for this structure gave one negative force constant. A visualization of the corresponding vibration, by using VIBRAM [13], agreed with the reaction coordinate expected from the dashed lines drawn in the structure of T_3 in Fig. 3. As a further test of T_3 an intrinsic reaction coordinate

Table 5
ROHF, MRCI, and ZPE energy values in Hartree for the different electronic states of the structures involved in the isomerization of the benzene radical cation to the Dewar benzene structure. Except for the transition state T_8, all values are calculated for the lowest state in C_{2v} symmetry. The relative energies in kcal mol^{-1} are given in Fig. 10. I_{sym} refers to the minimum geometry obtained by an optimization in C_{2v} symmetry after symmetrization of transition state T_8 (see text)

	Symmetry	ROHF	MRCI	ZPE
Benzene $1^{\cdot+}$	b_2	−230.421222	−230.868602	0.105319
	b_1		−230.851396	
	a_1		−230.763379	
	a_2		−230.748119	
I_{sym}	a_1	−230.288110	−230.733720	0.102490
	b_1		−230.662497	
	b_2		−230.656325	
	a_2		−230.632751	
T_8		−230.280288	−230.728065	0.101090
Dewar benzene$^{\cdot+}$	b_1	−230.291858	−230.739705	0.100975
	a_1		−230.675009	
	a_2		−230.632892	
	b_2		−230.630242	

(IRC) calculation was done by using a 4-31G basis set. This calculation indeed showed a connection of T_3 with both structures **2** and **10**.

Dissociation of structure **10** via the transition state T_4 leads to a shallow minimum that can be ascribed to the ion induced dipole attraction and from this minimum to the separated fragments, that at a distance of 15 Å have an energy slightly below the energy of T_4 (Table 3). The final energy diagram is shown in Fig. 4. In this energy diagram the total energy of the separated fragments is set equal to the value at 15 Å.

3.2. Possible fragmentation pathways to the vinyl acetylene structure

In [9], it was suggested that the most probable way for the formation of the vinyl acetylene fragment radical cation is the breaking of two C–C bonds in structure **3**. This mechanism was first tested by a semiempirical (PM3) grid calculation in which the C_1–C_6 and C_4–C_5 distances were varied. The resulting potential energy surface is shown in Fig. 5.

Fig. 5 suggests that there are two possible pathways of comparable energy. In path A (Fig. 5) an increase of the C_4–C_5 distance leads to an almost flat part of the potential energy surface from which the separated fragments can be reached. In path B the reaction goes via a breaking of the C_1–C_6 bond to form the intermediate structure **14** and, subsequently, a breaking of the C_4–C_5 bond. The corresponding reaction schemes are shown in Fig. 6 and the results of the ab initio calculations are given in Table 4. It should be noted that the relative orientation of the fragments in **13** and **13′** (Fig. 6) is different. For this reason there is a small difference in the calculated energies.

The calculations again show that dissociation proceeds via a minimum that can be ascribed to the ion induced dipole attraction. An interesting point, furthermore, is that, in contrast to the semiempirical and ROHF results, the energy of structure **12** is higher than the energy of transition state T_5. This shows that, as assumed in the reaction scheme in Fig. 6(a), **12**, indeed, is not an intermediate in path A (Fig. 5). An (ROHF) IRC calculation by using a 4-31G basis set, nevertheless, produced structure **12** as the product ion. We consider this to be an artefact caused by the fact that at the ROHF level the energy of **12** is lower than that of T_5. In fact, an optimization starting with a geometry from the IRC calculation close to T_5 produced structure **3** instead of **12**.

The energy diagrams for the fragmentations via path A and B are shown in Fig. 7 where, again, the energy of the separated fragments is set equal to the

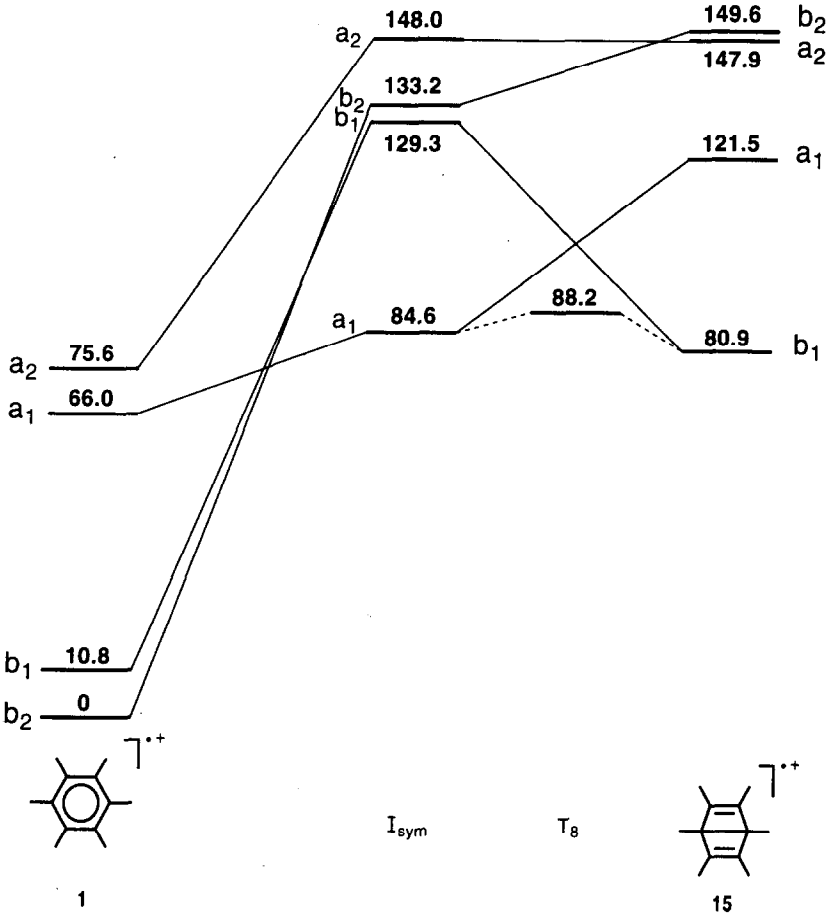

Fig. 10. Correlation diagram for the rearrangement of the benzene radical cation to the Dewar benzene structure.

value at 15 Å. In the present case, the minima between the final transition state and the fragments are only obtained at the ROHF level. After the MRCI calculation T_5 in path A is only 0.4 kcal mol^{-1} above the minimum, whereas in path B T_7 is even slightly below the ROHF minimum. The barriers in the two possible pathways are essentially identical, but a fragmentation along path A is somewhat more direct and for this reason perhaps more likely.

3.3. A possible fragmentation pathway to the cyclobutadiene structure

As noted above, the only reasonable precursor for a fragmentation to the cyclobutadiene structure seems

Table 6
ROHF, MRCI, and ZPE energy values in Hartree for the radical cation structures and transition states in Fig. 11 and relative energies with respect to the benzene structure in kcal mol^{-1}. The latter values are obtained from the MRCI energies corrected for the ROHF zero-point energies scaled by a factor of 0.89

	ROHF	ZPE	MRCI	ΔE
Benzene $\mathbf{1}^{\cdot+}$ [a]	−230.421222	0.105319	−230.868588	0
T_8	−230.280288	0.101090	−230.728065	85.8
Dewar benzene$^{\cdot+}$	−230.291858	0.100975	−230.739705	78.4
T_9	−230.259187	0.100627	−230.719191	91.1
Structure **16**	−230.288477	0.101628	−230.725192	87.9
T_{10}	−230.231216	0.096693	−230.685201	110.3
17, minimum	−230.244159	0.094194	−230.685921	108.4
10 Å	−230.236603	0.093474	−230.676278	114.1
15 Å	−230.236374	0.093093	−230.676207	113.9

[a]Values taken from [5].

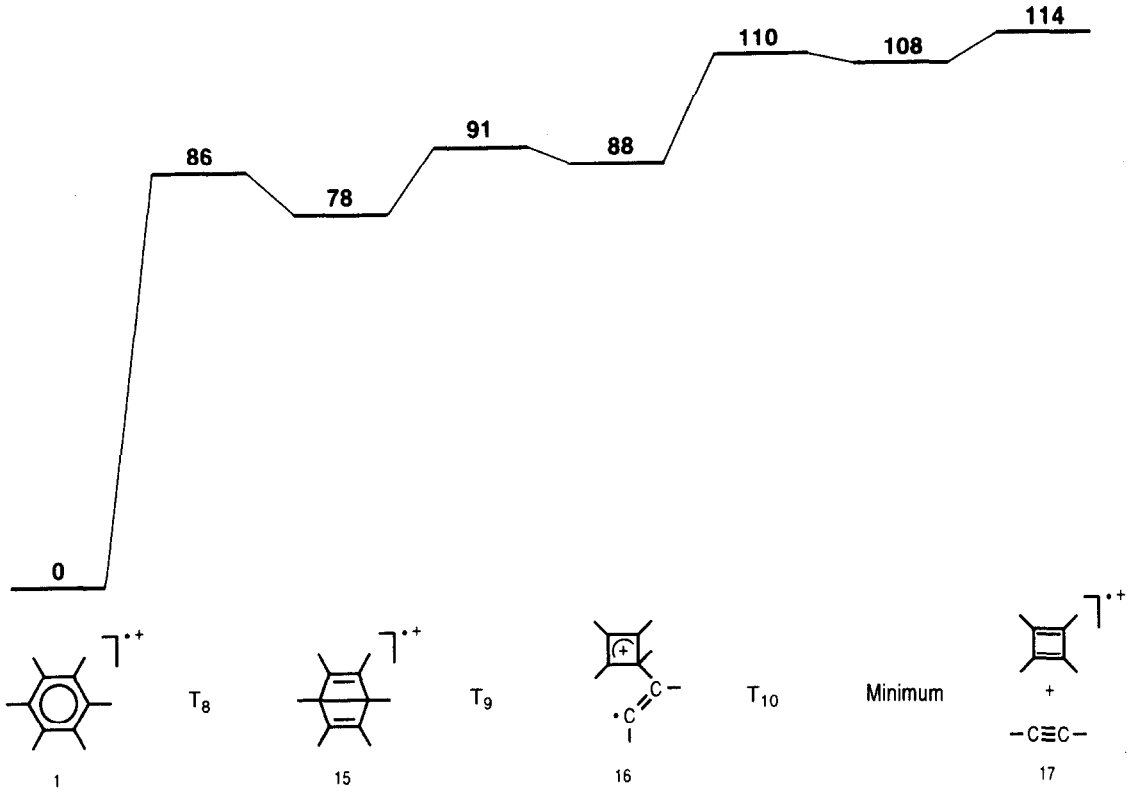

Fig. 11. Energy diagram for the fragmentation to the cyclobutadiene structure. The relative energies are in kcal mol^{-1}.

to be the Dewar benzene structure. This leads to the reaction scheme shown in Fig. 8.

In the following, we will first consider the first step, the isomerization to the Dewar benzene structure, and, subsequently, the dissociation of this latter ion structure.

It is well known that the formation of neutral Dewar benzene from the benzene molecule is forbidden in the sense of the Woodward–Hoffmann rules [18]. This is easily seen from the benzene π-electron molecular orbitals (MOs) shown in Fig. 9(a). Orbital Φ_3, which is doubly occupied in benzene, correlates with an unoccupied MO in Dewar benzene, whereas the reverse holds for MO Φ_5. ROHF calculations

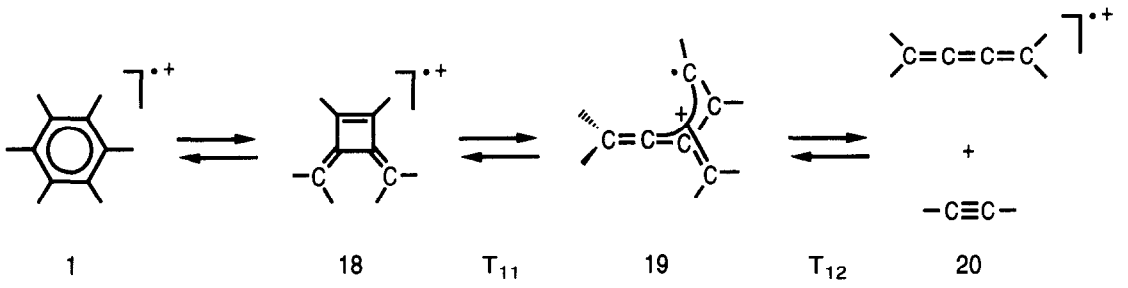

Fig. 12. Reaction scheme for the fragmentation to the butatriene radical cation.

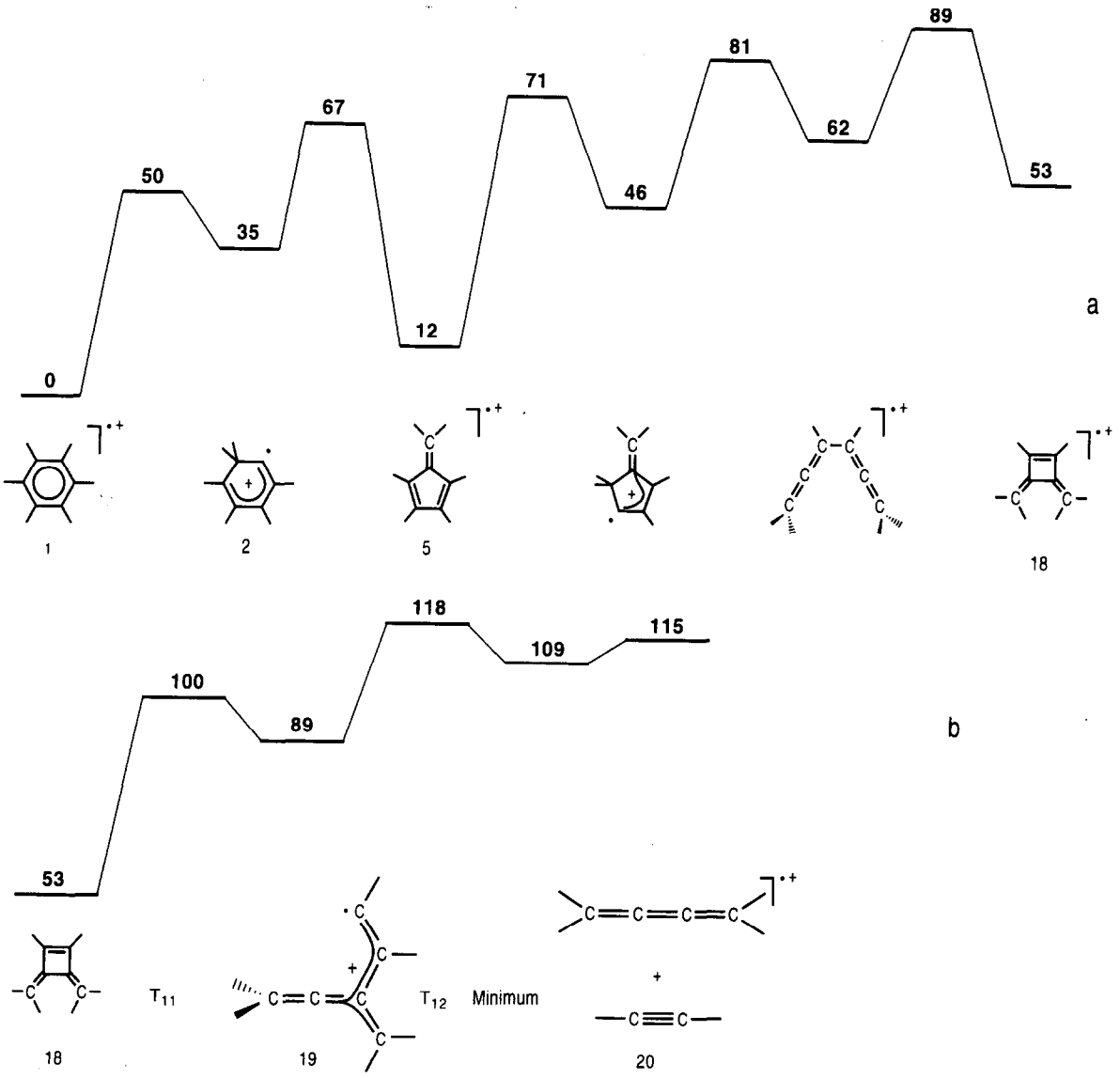

Fig. 13. Energy diagram for the isomerization of the benzene radical cation to the dimethylene cyclobutene structure (a) [7] and for the dissociation of the latter structure to the butatriene fragment ion. The relative energies are in kcal mol^{-1}.

show that the change in orbital occupation is more complex in the case of the radical cations [Fig. 9(b)]. The unpaired electron in the Dewar benzene radical cation is in the orbital that correlates with the doubly occupied benzene MO Φ_2 (symmetry b_1 in C_{2v}). The unoccupied benzene MO Φ_5 becomes doubly occupied in the Dewar benzene radical cation and the singly occupied MO Φ_3 (symmetry b_2 in C_{2v}) will be unoccupied after isomerization. It follows from Fig. 9(b) that an isomerization of the benzene radical cation to the Dewar benzene structure is probably determined by two curve crossings and that it is rather likely that the transition state will be asymmetric because of an avoided crossing. The transition state T_8

Table 7
ROHF, MRCI, and ZPE energy values in Hartree for the radical cation structures and transition states in Figs. 12 and 13 and relative energies with respect to the benzene structure in kcal mol^{-1}. The latter values are obtained from the MRCI energies corrected for the ROHF zero-point energies scaled by a factor of 0.89

	ROHF	ZPE	MRCI	ΔE
Benzene **1**$^{\cdot+}$ [a]	−230.421222	0.105319	−230.868588	0
Dimethylene cyclobutene **18**$^{\cdot+}$ [a]	−230.333331	0.101906	−230.780686	53.3
T_{11}	−230.246767	0.096437	−230.701199	100.1
Structure **19**	−230.280953	0.098024	−230.720901	88.6
T_{12}	−230.222377	0.093323	−230.669536	118.2
20, minimum	−230.235918	0.092992	−230.684175	108.8
10 Å	−230.230100	0.091823	−230.673475	114.9
15 Å	−230.229784	0.091793	−230.673174	115.1

[a]Values taken from [5] and [7].

indeed appeared to be asymmetric. If the geometry of T_8 is optimized after symmetrization in C_{2v}, the result is an ion structure (I_{sym} in Fig. 10 and Table 5), where the unpaired electron is in an orbital of a_1 symmetry in C_{2v} correlating with Φ_5 in benzene as may be expected from Fig. 9(b). In order to get a more complete picture of the isomerization of the benzene radical cation to the Dewar benzene structure the lowest states of all possible symmetries have been calculated for the benzene, I_{sym} and Dewar benzene radical cations. The resulting energies are given in Table 5 and the corresponding correlation diagram is presented in Fig. 10. In this diagram the position of T_8 is based on the differences in the length of the central bond with the lengths in I_{sym} and in the Dewar radical cation. This position clearly shows that T_8 depends on an avoided crossing of potential energy surfaces of a_1 and b_1 symmetry as one may expect from Fig. 9(b).

The calculation of the dissociation of the Dewar benzene radical cation appeared to be relatively straightforward. The resulting energies are given in Table 6 and the corresponding energy diagram is shown in Fig. 11. Also in this case, dissociation proceeds via a minimum.

Table 8
Relative energies in kcal mol^{-1} with respect to the benzene radical cation of the highest barriers and the separated fragments for the pathways studied

Fragment	Highest barrier	Fragments
Methylene cyclopropene$^{\cdot+}$	105	103
Vinyl acetylene$^{\cdot+}$ path A	114[a]	114
$^{\cdot+}$ path B	113	114
Cyclobutadiene$^{\cdot+}$	114[a]	114
Butatriene$^{\cdot+}$	118	115

[a]The highest isomerization barrier is lower than or essentially equal to the energy of the separated fragments.

3.4. A possible fragmentation pathway to the butatriene structure

As remarked above, the most reasonable pathway for a fragmentation to the butatriene structure probably is an isomerization to the dimethylene cyclobutene radical cation **18** followed by a dissociation of the latter ion (Fig. 12). The first step, the isomerization to the dimethylene cyclobutene structure, has been discussed in a previous article [7]. In that work,

Table 9
Energies of C_4H_4 fragment radical cations relative to the energy of the methylenecyclopropene radical cation in kcal mol^{-1}. The calculations in [9] are on the MRCI/ROHF//6-31G** level as in the present work. In the DFT and QCISD calculations in [20] a 6-31G* basis set was used and the CCSD(T) calculations were done with Dunning's correlation-consistent triple-zeta basis set [21] at the QCISD geometry

	Vinyl acetylene$^{\cdot+}$	Cyclobutadiene$^{\cdot+}$	Butatriene$^{\cdot+}$
Present work	10	11	12
[9]	11	9	6
DFT [20]	8	10	2
QCISD [20]	11	10	9
CCSD(T) [20]	10	7	7

the isomerization barrier was calculated to be 89 kcal mol^{-1}, which is lower than the experimental value for the dissociation considered. The energy diagram for this process is shown in Fig. 13(a). The calculated energy values for the dissociation of the dimethylene cyclobutene radical cation are given in Table 7 and the corresponding energy diagram is shown in Fig. 13(b).

4. Conclusions

The maximum barriers and the energies of the separated fragments for the different pathways studied are summarized in Table 8. It is quite clear that the dissociation of lowest energy is the formation of the methylene cyclopropene fragment ion as assumed previously [2,3]. The calculated barrier of 105 kcal mol^{-1} is somewhat higher than the experimental value of 96 kcal mol^{-1} given in [16] but the energy of the separated fragments of 103 kcal mol^{-1} is very close to the values recently obtained in [19]. In that work the authors obtained a value of 105.8 kcal mol^{-1} for the energy difference between the benzene radical cation and the separated fragments from density functional (DFT) calculations and of 102.6 kcal mol^{-1} at the CCSD(T) level (coupled cluster calculations with single and double substitutions and a noniterative inclusion of triple excitations). For a fragmentation to the other classical C_4H_4 ion structures both the barriers and the energies of the separated fragments are highly comparable. Also in previous calculations these C_4H_4 radical cations were found to have almost equal energies, although there is some scatter in the results for the butatriene cation (Table 9). In this latter case, the DFT energy in particular seems rather low. From all these results together, we conclude that the experimental finding [2] that, besides the methylene cyclopropene ion, only the vinyl acetylene ion is observed in fragmentations of C_6H_6 precursors cannot be ascribed to differences in barriers along the possible dissociation pathways but should be caused by the fact that the transition states for a formation of the vinyl acetylene ion structure are much closer to the benzene structure than the transition states for formation of the other classical C_4H_4 fragment ions. The vinyl acetylene ion is obtained by fragmentation of structure **3**, which is connected with the benzene structure via two barriers of relatively low energy (Fig. 7), whereas for the cyclobutadiene and butatriene fragments a number of barriers of high energy have to be passed (Figs. 11 and 13).

References

[1] T. Baer, in The Structure, Energetics, and Dynamics of Organic Ions, T. Baer, C. Y. Ng, I. Powis (Eds.), Wiley, Chichester, 1996, 143.
[2] M.-Y. Zhang, B.K. Carpenter, F.W. McLafferty, J. Am. Chem. Soc. 113 (1991) 9499.
[3] B.J. Shay, M.N. Eberlin, R.G. Cooks, and C. Wesdemiotis, J. Am. Soc. Mass Spectrom. 3 (1992) 518.
[4] W.J. van der Hart, Int. J. Mass Spectrom. Ion Processes 130 (1994) 173.
[5] W.J. van der Hart, J. Am. Soc. Mass Spectrom. 6 (1995) 513.
[6] W.J. van der Hart, J. Am. Soc. Mass Spectrom. 7 (1996) 731.
[7] W.J. van der Hart, J. Am. Soc. Mass Spectrom. 8 (1997) 594.
[8] W.J. van der Hart, J. Am. Soc. Mass Spectrom. 8 (1997) 599.
[9] G. Koster and W.J. van der Hart, Int. J. Mass Spectrom. Ion Processes 163 (1997) 169.
[10] M.F. Guest, P. Fantucci, R.J. Harrison, J. Kendrick, J.H. van Lenthe, K. Schoeffel, and P. Scherwood, GAMESS-UK User's Guide and Reference Manual, Revision C.0, Computing for Science (CFS) Ltd., Daresbury Laboratory, Daresbury, UK, 1992.
[11] M.J. Frisch, G.W. Trucks, H.B. Schlegel, P.M.W. Gill, B.G. Johnson, M.A. Robb, J.R. Cheeseman, T. Keith, G.A. Petersson, J.A. Montgomery, K. Raghavachari, M.A. Al-Laham, V.G. Zakrzewski, J.V. Ortiz, J.B. Foresman, J. Cioslowski, B.B. Stefanov, A. Nanayakkara, M. Challacombe, C.Y. Peng, P.Y. Ayala, W. Chen, M.W. Wong, J.L. Andres, E.S. Replogle, R. Gomperts, R.L. Martin, D.J. Fox, J.S. Binkley, D.J. Defrees, J. Baker, J.P. Stewart, M. Head-Gordon, C. Gonzalez, J.A. Pople, Gaussian 94, Revision B.1, Gaussian, Inc., Pittsburgh, PA, 1995.
[12] W.J. van der Hart, Int. J. Mass Spectrom. Ion Processes 151 (1995) 27.
[13] J. Dillen, Program No. QCMP 12010, Quantum Chemistry Program Exchange, Indiana University, Bloomington, IN, 1992.
[14] R.J. Buenker, R.A. Philips, J. Mol. Struct. (Theochem) 123 (1985) 291.
[15] S.T. Elbert, E.R. Davidson, Int. J. Quantum Chem. 8 (1974) 857.
[16] H. Kühlewind, A. Kiermeier, H.J.J. Neusser, J. Chem. Phys. 85 (1986) 4427.
[17] S.J. Klippenstein, J.D. Faulk, R.C. Dunbar, J. Chem. Phys. 96 (1993) 243.
[18] R.B. Woodward, R. Hoffmann, The Conservation of Orbital Symmetry, Verlag Chemie, Weinheim, 1970.
[19] Y. Ling, J.M.L. Martin, C. Lifshitz, J. Phys. Chem. A 101 (1997) 219.
[20] V. Hrouda, M. Roeselová, T. Bally, J. Phys. Chem. A 101 (1997) 3925.
[21] T.H. Dunning, J. Chem. Phys. 90 (1989) 1007.